The American Journal of Pathology, Vol. 174, No. 4, April 2009

DOI: 10.2353/ajpath.2009.080697

Gastrointestinal, Hepatobiliary and Pancreatic Pathology

Oxidative Stress-Mediated Mitochondrial Dysfunction Contributes to Angiotensin II-Induced Nonalcoholic Fatty Liver Disease in Transgenic Ren2 Rats

Yongzhong Wei,*† Suzanne E. Clark,*† John P. Thyfault,*† Grace M.E. Uptergrove,*† Wenhan Li,*† Adam T. Whaley-Connell,*† Carlos M. Ferrario,‡ James R. Sowers,*† and Jamal A. Ibdah*†

From the Department of Internal Medicine, University of Missouri School of Medicine, Columbia, Missouri; the Harry Truman Veterans Administration Medical Center,† Columbia, Missouri; and Wake Forest University School of Medicine,‡ Winston-Salem, North Carolina*

Emerging evidence indicates that impaired mitochondrial fatty acid β-oxidation plays a key role in liver steatosis. We have recently demonstrated that increased angiotensin (ANG) II causes progressive hepatic steatosis associated with oxidative stress; however, the underlying mechanisms remain unclear. We hypothesized that ANG II causes hepatic mitochondrial oxidative damage and impairs mitochondrial β-oxidation, thereby leading to hepatic steatosis. We used the Ren2 rat with elevated endogenous ANG II levels to evaluate mitochondrial ultrastructural changes, gene expression levels, and β-oxidation. Compared with Sprague-Dawley littermates, Ren2 livers exhibited mitochondrial damage and reduced β-oxidation, as evidenced by ultrastructural abnormalities, decrease of mitochondrial content, percentage of palmitate oxidation to CO_2, enzymatic activities (β-HAD and citrate synthase), and the expression levels of cytochrome *c*, cytochrome *c* oxidase subunit 1, and mitochondrial transcription factor A. These abnormalities were improved with either ANG II receptor blocker valsartan or superoxide dismutase/catalase mimetic tempol treatment. Both valsartan and tempol substantially attenuated mitochondrial lipid peroxidation in Ren2 livers. Interestingly, there was no difference in the expression of key enzymes (ACC1 and FAS) for fatty acid syntheses and their transcription factors (SREBP-1c and ChREBP) between Sprague-Dawley, untreated Ren2, and valsartan- or tempol-treated Ren2 rats. These results document that ANG II induces mitochondrial oxidative damage and impairs mitochondrial β-oxidation, contributing to liver steatosis. ***(Am J Pathol 2009, 174:1329–1337; DOI: 10.2353/ajpath.2009.080697)***

Nonalcoholic fatty liver disease (NAFLD) is the most common liver disease in the US and significantly contributes to premature mortality.[1–4] NAFLD represents a wide spectrum of disorders ranging from liver steatosis, to steatohepatitis and cirrhosis, and increases the risk for development of hepatocellular carcinoma.[5,6] Importantly, liver steatosis is the first and critical step in NAFLD, which may progress to advanced steatohepatitis characterized by hepatocyte injury, inflammation and fibrosis, and ultimately end-stage cirrhosis.[2–4,7] However, the precise mechanisms for initiation and progression of NAFLD remain unclear.

Emerging evidence indicates that oxidative stress and inflammation may play a fundamental role in the pathogenesis of NAFLD.[2–4] Angiotensin (ANG) II, the primary component of the renin angiotensin system, has pro-oxidant, pro-inflammatory, and profibrogenic activities. ANG II plays an integral role in the pathogenesis of hypertension.[8] Clinical and experimental evidence suggests that ANG II is also implicated in liver disease.[9–18] Patients with cirrhosis and rats with active liver fibrogenesis exhibit increased systemic ANG II levels and local hepatic renin angiotensin system activity.[11,14] Animals with liver steatosis have increased expression of ANG II and ANG II type 1 receptor (AT_1R) in the livers.[12,13,17] ANG II inhibition has been shown to attenuate triglyceride (TG) accumulation in the liver of Zucker obese rats.[15,17]

Supported in part by the National Institutes of Health (grants RO1-DK-56345 to J.A.I. and RO1-HL073101 to J.R.S.), the Novartis Pharmaceutical Co. (to J.R.S.), and the University of Missouri Research Council (to Y.W.).

Accepted for publication December 30, 2008.

Address reprint requests to Jamal A. Ibdah, M.D., Ph.D., Division of Gastroenterology and Hepatology, Department of Internal Medicine, University of Missouri–Columbia, Columbia, MO 65212. E-mail: ibdahj@health.missouri.edu.

We have recently reported that ANG II causes progressive hepatic steatosis, inflammation, and fibrosis associated with oxidative stress in a transgenic Ren2 rat model with elevated endogenous ANG II levels.[18] These observations suggest that ANG II plays a role in the initiation and progression of NAFLD. However, the underlying mechanisms of ANG II-induced hepatic TG accumulation remain to be elucidated. Many factors have been implicated in liver steatosis, increased fatty acid syntheses through activation of lipogenic pathway and/or decreased fatty acid oxidation represent two critical mechanisms in triggering hepatic TG accumulation.[2–4]

Mitochondrial β-oxidation is the major pathway for fatty acid oxidation. Emerging evidence indicates that impaired mitochondrial β-oxidation plays a key role in liver steatosis.[4] Mitochondria are rich in proteins and enzymes encoded by both nuclear and mitochondrial DNA (mtDNA). mtDNA is more vulnerable to damage than nuclear DNA by a variety of pathological insults including reactive oxygen species (ROS).[19] Accordingly, we hypothesize that increased ROS by ANG II causes mitochondrial oxidative damage, leading to depletion and/or reduction of mitochondrial genes and proteins, impaired mitochondrial β-oxidation, and consequently development of hepatic steatosis. We further hypothesize that AT_1R blockade and/or antioxidant treatment will attenuate mitochondrial oxidative damage and improve hepatic mitochondrial gene and protein expression, as well as hepatic mitochondrial β-oxidation in this Ren2 rat model.

Materials and Methods

Animals and Treatment

Male Sprague-Dawley (SD) and transgenic heterozygous (+/−) Ren2 rats were received from Wake Forest University School of Medicine (Winston-Salem, NC). All rats were maintained on Formulab Diet (5008; PMI Nutrition International, LLC, Brentwood, MO) with free access to drinking water. SD and Ren2 rats at the age of 9 weeks were randomly assigned as untreated SD control (SD), Ren2 control (RC), Ren2 valsartan (RV), and Ren2 tempol (RT) (six to seven rats in each group). Rats were given valsartan at 30 mg/kg/day or tempol at 1 mmol/L in their drinking water or placebo for 3 weeks. All animal procedures followed the University of Missouri Animal Care and Use Committees and National Institutes of Health guidelines.

Materials

The AT_1R blocker (valsartan) was supplied by Novartis Pharmaceutical Co. (East Hanover, NJ) and the superoxide dismutase (SOD)/catalase mimetic (tempol) was purchased from Sigma-Aldrich Co. (St. Louis, MO). Antibodies against SREBP-1c, ChREBP, FAS, ACC1, CPS1, MTCO1, cytochrome *c*, mtTFA were obtained from Cell Signaling (Danvers, MA), Abcam (Cambridge, MA), BD Bioscience (San Jose, CA), Santa Cruz Biotechnology (Santa Cruz, CA), and Upstate (Lake Placid, NY), respectively.

Transmission Electronic Microscopy

Liver tissues were collected and fixed in 2% glutaraldehyde/2% paraformaldehyde, and secondary fixation with 1% osmium tetroxide, embedded in Epon-Spurr's resin, sectioned at 85 nm, and stained with uranyl acetate/Sato's triple lead stain. Electron microscopy was performed at the University of Missouri–Columbia Electron Microscopy Core Facility using a JEOL (Tokyo, Japan) 1200-EX transmission electron microscope.

Immunohistochemistry

Liver paraffin sections were deparaffinized and nonspecific antibody binding was blocked with 5% bovine serum albumin and 5% goat or rabbit serum in phosphate-buffered saline. These sections were incubated with anti-CPS1, ChREBP, or SREBP-1c antibodies at 1:200 dilutions for overnight at 4°C. After washing, the sections were incubated with a second antibody conjugated with Alexa-486 or -568 for 1 hour at room temperature. The sections were counterstained with 4,6-diamidino-2-phenylindole (DAPI) (Vector Laboratories, Burlingame, CA) and mounted with mounting media (Vector Laboratories). Images were acquired with a fluorescence microscope (Eclipse 50i; Nikon, Tokyo, Japan).

Measurement of Mitochondrial Oxidative Stress

4-HNE, a by-product of lipid peroxidation and a marker of oxidative stress, was measured by Western blot. Liver samples were homogenized using a tissue homogenizer (Retsch, Newtown, PA) in lysis buffer [50 mmol/L phosphate buffer, 0.01 mmol/L ethylenediaminetetraacetic acid, 1 mmol/L phenylmethyl sulfonyl fluoride, 2 μmol/L leupeptin, and 2 μmol/L pepstatin A (pH 7.4)]. The homogenate was centrifuged at 1000 $\times$ *g* for 30 minutes at 4°C, and the supernatant (S1) was further centrifuged at 13,000 $\times$ *g* for 20 minutes at 4°C, yielding supernatant (S2) and a pellet containing mitochondria. Forty μg of protein (mitochondrial fractions) were loaded in a sodium dodecyl sulfate-polyacrylamide gel electrophoresis and transferred to a polyvinylidene difluoride membrane and probed with anti-4-HNE antibodies (1:1000 dilution) against 4-HNE-modified proteins. After washing, the membrane was incubated with horseradish peroxidase-conjugated secondary antibodies (1:10,000 dilution). The signal was captured using a Phospho-imager system (Bio-Rad, Hercules, CA) and the intensities of the immunoblot bands were quantified using Quantity One software (Bio-Rad). β-Actin was used as a loading control.

SOD Activity

Liver samples were homogenized in a buffer (0.25 mol/L sucrose, 0.5 mmol/L ethylenediaminetetraacetic acid, 50

mmol/L HEPES, protease inhibitors, and phosphatase inhibitors). The homogenate was centrifuged at 1500 × *g* for 5 minutes at 4°C. The supernatant was used for measuring cytosolic Cu-ZnSOD activity using a commercial kit (OxisResearch, Foster City, CA). The supernatant was treated with 2 mmol/L potassium cyanide to inhibit both Cu/Zn-SOD and extracellular SOD and used for measuring mitochondrial MnSOD activity using a commercial kit (Cayman Chemical Co., Ann Arbor, MI).

Real-Time Polymerase Chain Reaction (PCR) Analysis

Total RNA was extracted using an RNA isolation kit (Qiagen, Valencia, CA) according to the manufacturer's instructions. Real-time PCR analysis was used to quantify expression levels of several key genes related to mitochondrial function in liver using an ABI Prism 7700 detector (PE Applied Biosciences, Foster City, CA): mitochondrial transcription factor A (mtTFA) using primers, forward: 5′-CAAGGGAAATTGAAGCTTGT-3′, reverse: 5′-CATTTGCTCTTCCCAAGACT-3′. Cytochrome *c* oxidase subunit 1 (MTCO1): forward, 5′-AGCAGGAATAGTAGGGACAGC-3′, reverse, 5′-TGAGAGAAGTAGTAGGACGGC-3′. For the analysis, 100 ng of total RNA were used, each sample was run in duplicate, and the mean value was used to calculate the gene expression level. Gene expression levels were normalized relative to the expression of housekeeping gene GAPDH.

Western Blot Analysis

Liver samples were homogenized as described above. Twenty-five μg of protein (whole homogenate) were loaded in a sodium dodecyl sulfate-polyacrylamide gel electrophoresis and transferred to a polyvinylidene difluoride membrane and probed with primary antibodies (1:1000) against CPS1, mtTFA, MTCO1, cytochrome *c*, FAS, ACC1, SREBP, and ChREBP. After washing, the membrane was incubated with horseradish peroxidase-conjugated secondary antibodies (1:10,000). The intensities of the bands were quantified as described above.

Enzyme Activity Assay

Enzyme activity for citrate synthase and β-hydroxyacyl-CoA dehydrogenase (β-HAD) was determined using a spectrophotometer at a wavelength of 412 nm and 340 nm, respectively, as described previously from our group.[20] Enzyme activity is expressed as U/ml/g protein.

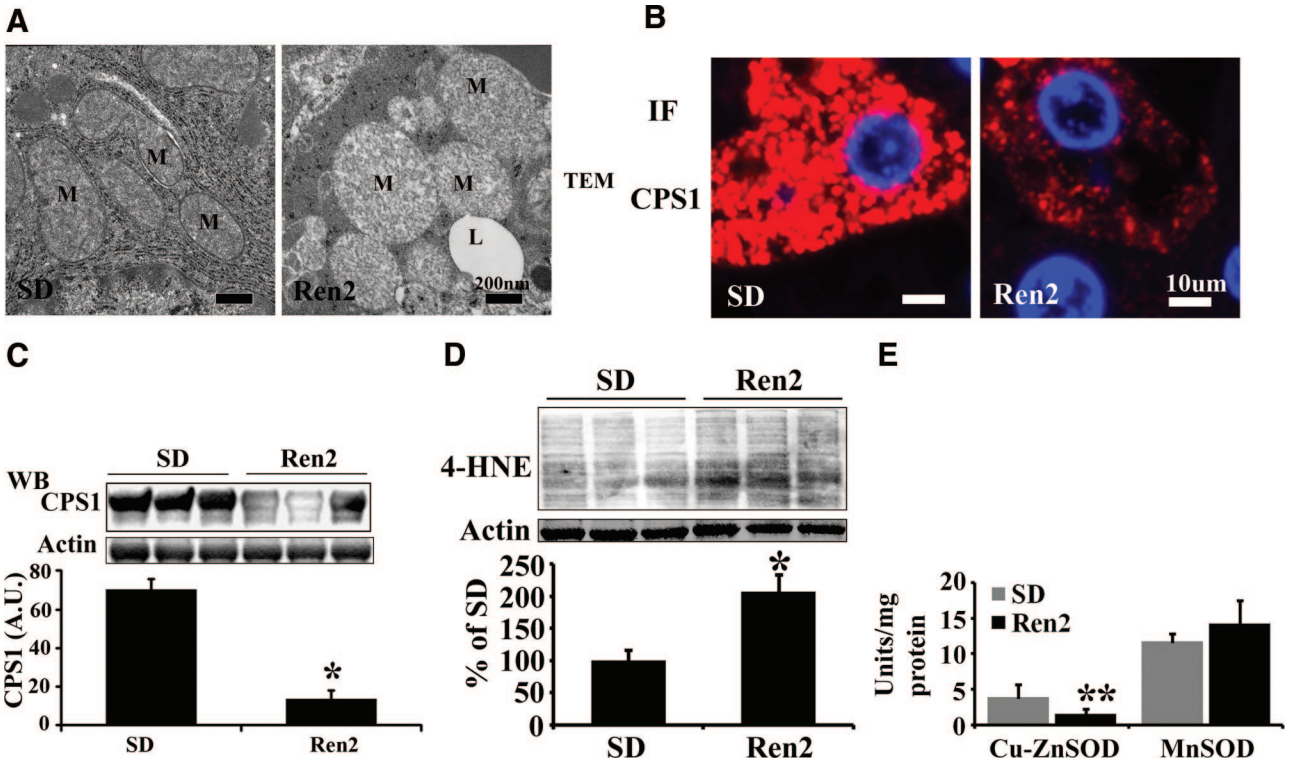

Figure 1. Mitochondrial morphology and content in livers from Ren2 and SD rats. **A:** Representative microphotographs of transmission electron microscopy, Ren2 livers showed big, swollen mitochondria with decreased matrix density compared with SD rats. M, mitochondria; L, lipid droplet. **B:** Representative immunofluorescence (IF) images showed decreased CPS1 (red) in Ren2 liver sections compared with SD controls. DAPI staining (blue) for nuclei. **C:** Representative immunoblot analyses for CPS1 (**top**) and bars representing band densitometry (**bottom**). **D:** Representative immunoblot analyses for 4-HNE (**top**) and bars representing band densitometry (**bottom**). **E:** Enzyme activities for cytosolic SOD (cu-znSOD) and mitochondrial SOD (mnSOD). The results are mean ± SEM for five rats for each group, $^{*}P < 0.01$ and $^{**}P < 0.05$ Ren2 versus SD. Scale bars: 200 nm (**A**); 10 μm (**B**). Original magnifications: ×25,000 (**A**); ×400 (**B**).

Fatty Acid Oxidation

Fatty acid oxidation was measured in the liver homogenate preparation as described previously from our group.[20] The oxidation rate of [^{14}C]palmitate was measured by collecting and counting the $^{14}CO_2$ and acid-soluble metabolites produced during incubation in a sealed trapping device. Palmitate (200 μmol/L) and [1-^{14}C]palmitate were bound to 0.5% bovine serum albumin (final concentration) at 37°C and brought up in reaction buffer to yield the following final concentrations: 100 mmol/L sucrose, 10 mmol/L Tris-HCl, 10 mmol/L KPO_4, 100 mmol/L KCl, 1 mmol/L $4MgCl_2 \cdot 6H_2O$, 1 mmol/L L-carnitine, 0.1 mmol/L malate, 2 mmol/L ATP, 0.05 mmol/L CoA, and 1 mmol/L dithiothreitol (pH 7.4). Reaction buffer (320 μl) was added to 80 μl of liver homogenate prepared in a sucrose-ethylenediaminetetraacetic acid buffer in the well of the trapping device. A 0.65-ml centrifuge tube containing 400 μl of NaOH also was inserted in the well followed by sealing the well with a rubber gasket. After 60 minutes of incubation at 37°C on an orbital shaker, 200 μl of 70% perchloric acid were injected through the rubber gasket into the bottom of the well. $^{14}CO_2$ driven out of the reaction by the perchloric acid during another 60-minute incubation was trapped in the NaOH and then counted on a scintillation counter. The remaining homogenate was centrifuged at 18,000 rpm for 20 minutes and a sample of the resulting supernatant (acid soluble metabolites) also was counted on a scintillation counter. Specific activity was taken by counting a portion of the reaction buffer.

Statistical Analysis

All data are reported as the means ± SEM. One-way analysis of variance test and Student's *t*-test were used to determine the significance among groups. A value of $P < 0.05$ was considered to be statistically significant.

Results

ANG II Contributes to Mitochondrial Damage in Ren2 Liver

We have recently demonstrated that Ren2 rats develop progressive hepatic steatosis.[18] Mitochondria play an integral role in lipid metabolism and homeostasis. To determine whether ANG II-induced hepatic steatosis is associated with mitochondrial damage, mitochondrial ultrastructure was assessed by transmission electronic microscopy, and mitochondrial content was determined by immunostaining and Western blot using an antibody against a hepatic mitochondrial marker carbamoyl-phosphate synthase (CPS)-1. Transmission electron microscopy analysis revealed mitochondrial ultrastructural abnormalities (swollen and reduced matrix density) in Ren2 livers compared with SD controls (Figure 1A). Immunostaining showed decreased CPS1 staining in Ren2 livers compared with SD rats (Figure 1B). Western blotting further corroborated significant reductions of CPS1 protein levels in Ren2 livers compared with SD (Figure 1C, $P < 0.01$).

In an earlier report, we have documented that ANG II induces NADPH oxidase activation and increases ROS formation in Ren2 livers.[18] To further determine whether increased ROS production contributes to mitochondrial oxidative stress, which in turn results in the mitochondrial abnormalities observed in Ren2 livers, mitochondrial fractions were insolated and lipid peroxidation was determined by measuring oxidative stress marker 4-HNE levels using Western blot analysis. Ren2 livers exhibited dramatically increased 4-HNE levels compared with SD controls (Figure 1D, $P < 0.05$). We further analyzed the activities of cytosolic SOD (Cu-ZnSOD) and mitochondrial SOD (Mn-SOD). Interestingly, Cu-ZnSOD, but not MnSOD activity, in Ren2 livers was markedly decreased compared with SD controls (Figure 1E).

ANG II Contributes to Depletion of Mitochondrial Genes and Proteins in Ren2 Liver

We analyzed the hepatic expression of mitochondrial genes and proteins including cytochrome *c* and mitochondrial cytochrome *c* oxidase subunit 1 (MTCO1). Expression of cytochrome *c* protein was markedly reduced in Ren2 livers compared with SD (Figure 2A). mRNA and

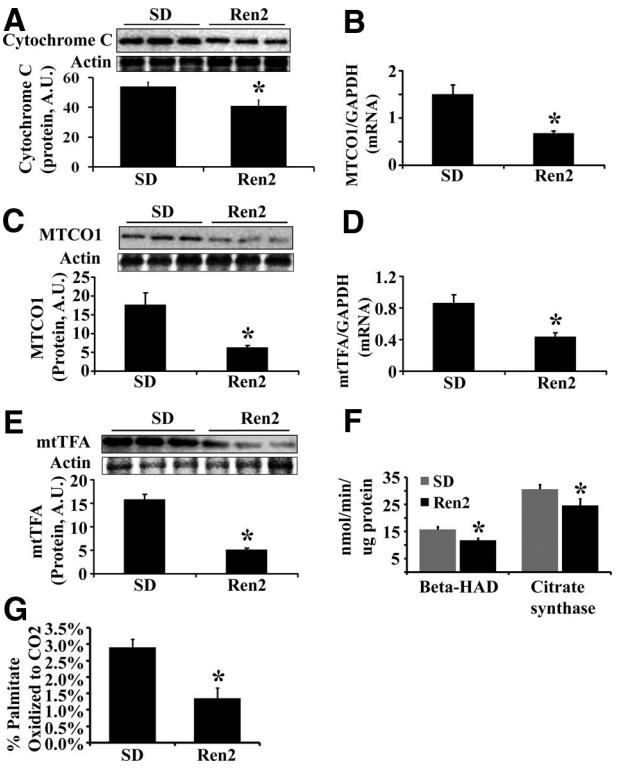

Figure 2. Hepatic mitochondrial indices and fatty acid β-oxidation. **A:** Representative immunoblot for cytochrome *c* (**top**) and bar graph for band densitometry (**bottom**). **B:** MTCO1 mRNA expression (normalized to GAPDH). **C:** Representative immunoblot for MTCO1 (**top**) and bar graph for band densitometry (**bottom**). **D:** mtTFA mRNA expression (normalized to GAPDH). **E:** Representative immunoblot band for mtTFA (**top**) and bars representing band densitometry (**bottom**). **F:** Activity of citrate synthase and β-HAD. **G:** The percentage of palmitate oxidized completely to CO_2. The results are mean ± SEM for five rats for each group, $^*P < 0.05$, Ren2 versus SD.

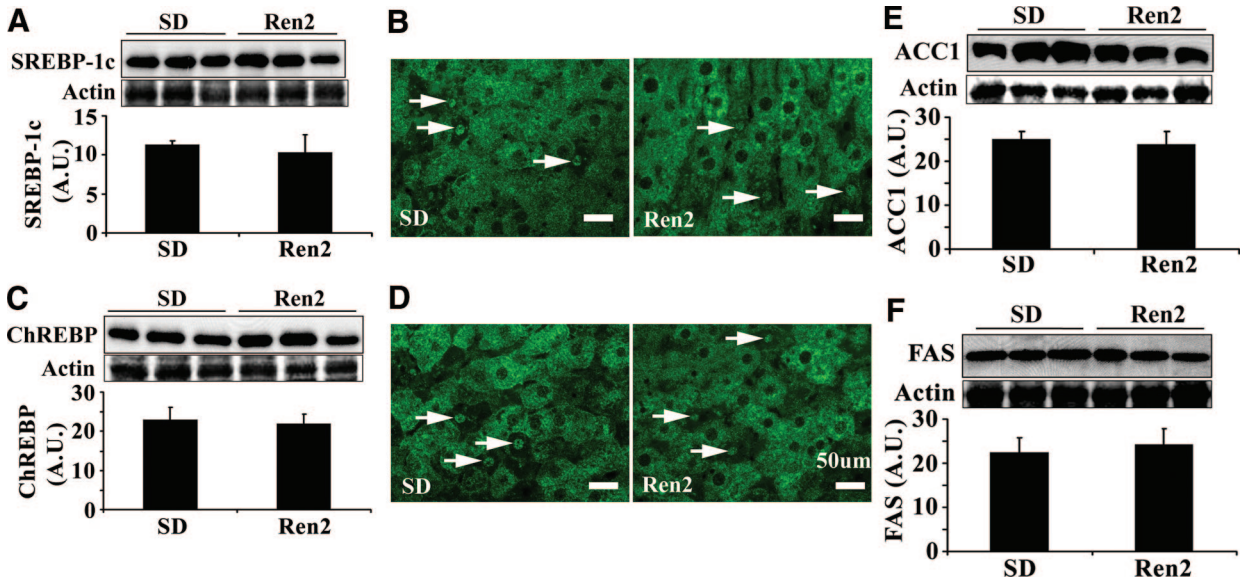

Figure 3. Hepatic lipogenic transcription factors and enzymes. **A:** Representative immunoblot for active SREBP-1c (68 kDa, **top**) and bar graph representing band densitometry (**bottom**). **B:** Representative immunofluorescence images showed that SREBP-1c was predominantly located in cytoplasm (green) and a few nuclei stained (**arrows**). **C:** Representative immunoblot for ChREBP (**top**) and bar graph representing band densitometry (**bottom**). **D:** Immunofluorescence staining for ChREBP. ChREBP was predominantly located in cytoplasm (green) and a few nuclei stained (**arrows**). **E** and **F:** Representative Western blot bands and densitometry analysis for ACC1 and FAS. The results of **A**, **C**, **E**, and **F** are mean ± SEM for five rats for each group, there were no significant differences between Ren2 versus SD controls ($P > 0.05$). No signal was obtained when liver sections were incubated with the secondary antibody only (data not shown). Scale bars = 50 μm. Original magnifications, ×400.

protein levels of MTCO1 were dramatically decreased in Ren2 livers compared with SD (Figure 2, B and C). Mitochondrial transcription factor A (mtTFA), an essential transcription factor in regulation of mitochondrial genes, at both mRNA and protein levels, was decreased in Ren2 livers compared with SD livers (Figure 2, D and E).

ANG II Impairs Mitochondrial β-Oxidation in Ren2 Liver

To evaluate mitochondrial fatty acid β-oxidation, the activities of β-hydroxyacyl-CoA dehydrogenase (β-HAD) and citrate synthase were measured and normalized to protein concentration. β-HAD is the rate limiting step for fatty acid β-oxidation in mitochondria. The activities (Figure 2F) and protein levels (data not shown) of β-HAD and citrate synthase were dramatically decreased in Ren2 livers compared with SD. Mitochondrial fatty acid β-oxidation was further determined by measuring the percentage of palmitate oxidized completely to CO_2. As shown in Figure 2G, there were markedly reduced palmitate oxidation in Ren2 livers compared with SD controls ($P < 0.05$).

ANG II Does Not Affect the Expression of Lipogenic Enzymes in Ren2 Liver

To determine whether ANG II-induced hepatic steatosis in Ren2 liver is associated with increased fatty acid synthesis, the key enzyme acetyl-CoA carboxylase (ACC1) and fatty acid synthase (FAS) as well as their transcription factors of SREBP-1c and ChREBP were analyzed by Western blot. There were no significant differences in the protein levels of active SREBP-1c (68 kDa, Figure 3A), total SREBP-1c (125 kDa, data not shown), and ChREBP (Figure 3C) between SD and Ren2 livers. Immunofluorescence revealed a similar staining pattern that SREBP-1c (Figure 3B) and ChREBP (Figure 3D) were predominantly located in the cytoplasm with a few stained nuclei in both Ren2 and SD livers. This further corroborated that there were comparable protein levels of ACC1 and FAS in Ren2 and SD livers (Figure 3, E and F).

AT_1R Blockade Attenuates Mitochondrial Damage and Improves Mitochondrial β-Oxidation in Ren2 Liver

The above data suggests that increased ANG II causes hepatic mitochondrial damage and impairs fatty acid β-oxidation, which contribute to the development of liver steatosis in the Ren2 rat model. To further determine whether ANG II inhibition protects hepatic mitochondria injury and improves mitochondrial β-oxidation, 9-week-old Ren2 rats were treated with the AT_1R blocker valsartan for 3 weeks. AT_1R blockade attenuated mitochondrial oxidative stress (Figure 4A), and enhanced cytosolic Cu-ZnSOD activity (Figure 4B) but not mitochondrial Mn-SOD activity (Figure 4B) compared with untreated Ren2 livers. Further, AT_1R blockade substantially increased mitochondrial content (Figure 4, C and D), cytochrome *c* protein (Figure 5A), MTCO1 mRNA (Figure 5B), MTCO1 protein (Figure 5C), mtTFA mRNA (Figure 5D), and mtTFA protein (Figure 5E) in treated Ren2 livers compared with untreated Ren2 controls. In addition, valsartan treatment dramatically attenuated the reduction of the activities of citrate synthase and β-HAD (Figure 5F) and

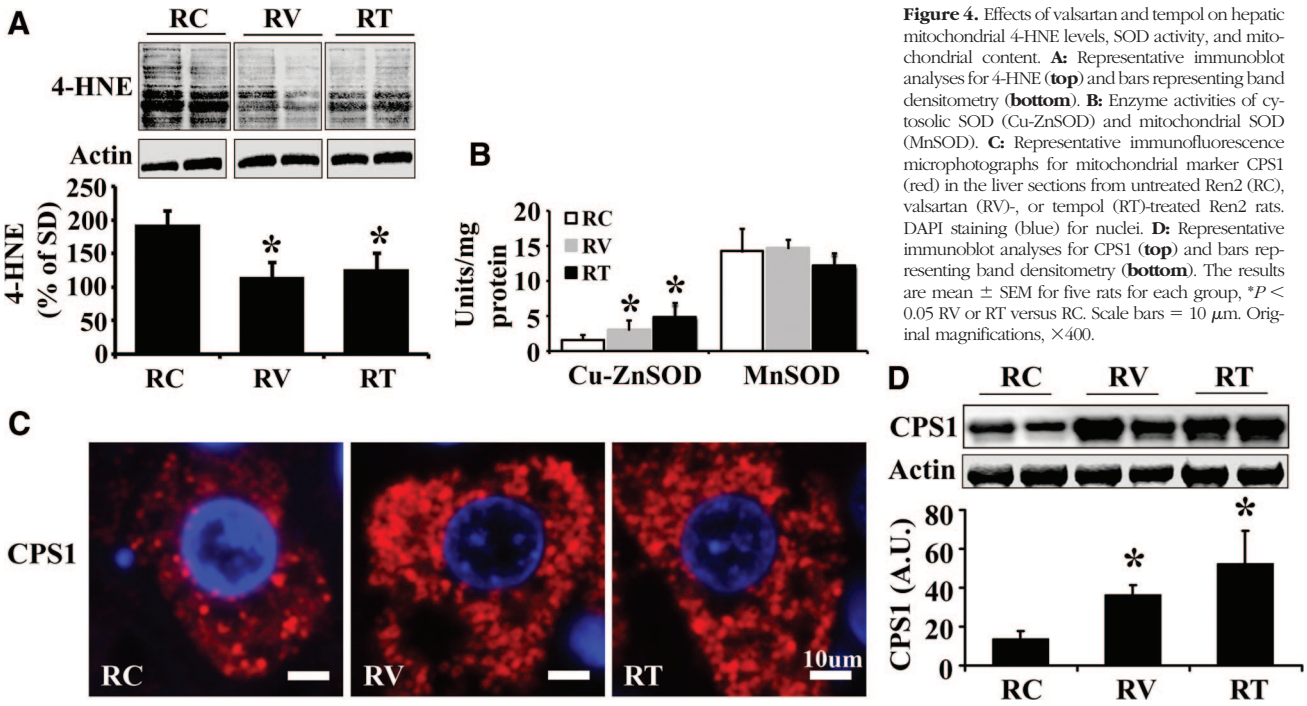

Figure 4. Effects of valsartan and tempol on hepatic mitochondrial 4-HNE levels, SOD activity, and mitochondrial content. **A:** Representative immunoblot analyses for 4-HNE (**top**) and bars representing band densitometry (**bottom**). **B:** Enzyme activities of cytosolic SOD (Cu-ZnSOD) and mitochondrial SOD (MnSOD). **C:** Representative immunofluorescence microphotographs for mitochondrial marker CPS1 (red) in the liver sections from untreated Ren2 (RC), valsartan (RV)-, or tempol (RT)-treated Ren2 rats. DAPI staining (blue) for nuclei. **D:** Representative immunoblot analyses for CPS1 (**top**) and bars representing band densitometry (**bottom**). The results are mean ± SEM for five rats for each group, $^*P <$ 0.05 RV or RT versus RC. Scale bars = 10 μm. Original magnifications, ×400.

the reduction in palmitate β-oxidation (Figure 5G) in the Ren2 livers, in conjunction with attenuation of hepatic steatosis in the Ren2 rats treated with valsartan.[18] These results suggest that ANG II-induced liver steatosis is attributable, at least in part, to ANG II-induced hepatic mitochondrial damage and impaired mitochondrial β-oxidation.

AT_1R Blockade Does Not Affect the Expression of Lipogenic Enzymes in Ren2 Liver

To determine whether AT_1R blockade affects the lipogenic pathway, ACC1, FAS, SREBP-1c, and ChREBP were analyzed by Western blot. There were no significant differences in the protein levels of active SREBP-1c (68 kDa, Figure 6A), total SREBP-1c (125 kDa, data not shown), and ChREBP (Figure 6B) between valsartan-treated and untreated Ren2 rats. Immunostaining showed a similar staining pattern of SREBP-1c and ChREBP in valsartan-treated and untreated Ren2 livers (data not shown). Similarly, there were no significant differences in the protein levels of ACC1 and FAS between valsartan-treated and untreated Ren2 rats (Figure 6, C and D).

Tempol Treatment Attenuates Mitochondrial Damage and Improves Mitochondrial β-Oxidation in Ren2 Liver

To further confirm that ANG II-impaired hepatic mitochondrial β-oxidation is mediated by oxidative stress, 9-week-old Ren2 rats were treated with the ROS scavenger tempol for 3 weeks. Tempol treatment attenuated mitochondrial lipid peroxidation (decreased 4-HNE levels) (Figure 4A), and enhanced cytosolic Cu-ZnSOD activities (Figure 4B), but not mitochondrial MnSOD activities (Figure 4B). Tempol treatment preserved mitochondrial content (Figure 4, C and D), the expression of cytochrome *c* (Figure 5A), MTCO1 mRNA (Figure 5B), MTCO1 protein (Figure 5C), mtTFA mRNA (Figure 5D), and mtTFA protein (Figure 5E) in the Ren2 livers. Tempol treatment substantially enhanced the activity of citrate synthase and β-HAD (Figure 5F) and palmitate β-oxidation (Figure 5G) compared with untreated Ren2 livers. In addition, as we reported earlier, tempol markedly attenuated hepatic steatosis in the Ren2 rat model.[18] These results further suggest that ANG II induces hepatic mitochondrial oxidative damage, which in turn impairs mitochondrial β-oxidation, consequently contributing to liver steatosis in Ren2 rat model.

Tempol Treatment Does Not Affect the Expression of Lipogenic Enzymes in Ren2 Liver

To determine whether tempol treatment affects the lipogenic pathways, ACC1, FAS, SREBP-1c, and ChREBP were analyzed by Western blot. Tempol treatment had no effect on the expression of active SREBP-1c (68 kDa, Figure 6A), total SREBP-1c (125 kDa, data not shown), and ChREBP (Figure 6B) compared with untreated Ren2 rats. Immunofluorescence showed a similar staining pattern of SREBP-1c and ChREBP between tempol-treated and untreated Ren2 livers (data not shown). There were no significant differences in the protein levels of ACC1 and FAS between tempol-treated and untreated Ren2 rats (Figure 6, C and D).

Discussion

Recent evidence suggests a strong relationship between hypertension and NAFLD.[21–23] ANG II is known to play a

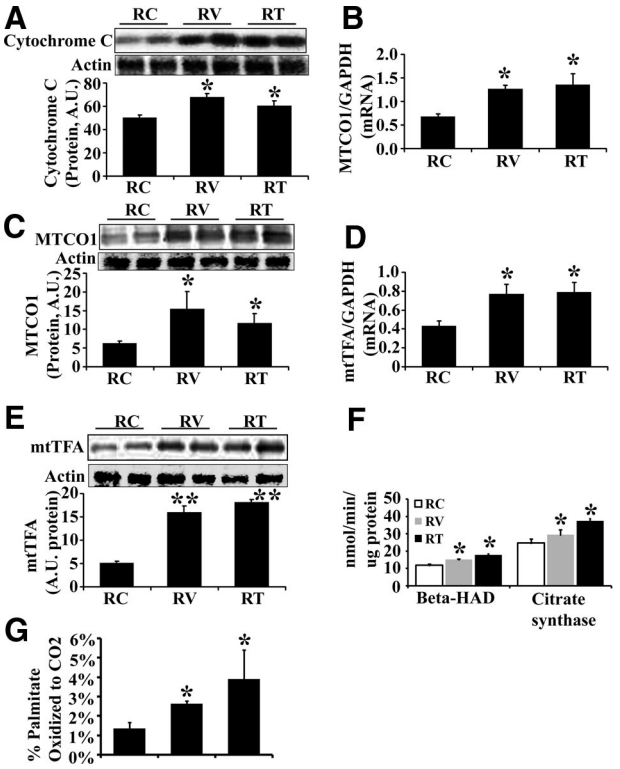

Figure 5. Effects of valsartan and tempol on hepatic mitochondrial indices and β-oxidation. **A:** Representative Western blot for cytochrome *c* (**top**) and bar graph for densitometry analysis (**bottom**). **B:** MTCO1 mRNA expression (normalized to GAPDH). **C:** Representative Western blot for MTCO1 (**top**) and bar graph for densitometry analysis (**bottom**). **D:** mtTFA mRNA expression (normalized with GAPDH). **E:** Representative Western blot for mtTFA (**top**) and bar graph for densitometry analysis (**bottom**). **F:** Activity of β-HAD and citrate synthase. **G:** The percentage of palmitate oxidized completely to CO_2. The results are mean ± SEM for five rats for each group, $^{*}P < 0.05$ RV or RT versus RC. $^{**}P < 0.01$ RV or RT versus RC.

critical role in the pathogenesis of hypertension. Emerging evidence indicates that ANG II is also implicated in the development of NAFLD.[12,13,17,18] For instance, ANG II levels are increased in the liver with fibrosis[11,14] and steatosis.[12,13,17] Further, ANG II inhibition ameliorates hepatic TG accumulation in Zucker obese rats[15,17] and renin angiotensin system-deficient mice are protected from high-fat diet-induced fatty liver disease.[24] ANG II infusion into normal rats induces hepatic steatosis that is dependent on the dose and duration of ANG II infusion.[16,25] Using a transgenic Ren2 rat model with elevated endogenous ANG II levels, we have recently demonstrated that ANG II causes progressive hepatic steatosis, inflammation, and fibrosis.[18] Furthermore, evidence suggests that ANG II-induced lipid accumulation in liver is likely to be associated with hepatic insulin resistance[13,26] and oxidative stress.[18] An *in vivo* study indicates that increased circulating ANG II by infusion induces hepatic insulin resistance[26] whereas inhibition of ANG II significantly attenuates hepatic insulin resistance and improves hepatic insulin signaling in animal models with fatty liver disease.[13] Collectively, these observations suggest that ANG II plays an important role in the pathogenesis of NAFLD. However, little is known regarding the mechanisms underlying ANG II-induced hepatic steatosis.

Our current investigation reveals a novel finding: increased ANG II levels cause mitochondrial oxidative damage, leading to depletion of mitochondrial genes and proteins, ultrastructural abnormalities, decreased mitochondrial content, and impaired mitochondrial β-oxidation. These mitochondrial abnormalities in Ren2 livers were substantially improved after valsartan or tempol treatment for 3 weeks. Hence, our results document that ANG II-mediated ROS formation induces mitochondrial abnormalities leading to reduced fatty acid oxidation, thereby contributing to the development of NAFLD. To our knowledge, this is the first study to report that ANG II induces hepatic mitochondrial oxidative damage and impairs mitochondrial β-oxidation, leading to ANG II-induced hepatic steatosis. Our results further extend our understanding that that NAFLD is a mitochondrial disease.[4,27–29] Indeed, patients and animals with NAFLD exhibit hepatic mitochondrial abnormalities at the morphological, molecular, and biochemical levels.[4,27,29,30] mtTFA is a critical transcription factor in regulation of mitochondrial genes, proteins, and functions. Indeed, mtTFA knockout mice display decreased expression of mitochondrial genes and protein, as well as mitochondrial dysfunction.[31] Our data document that there was decreased mtTFA expression in Ren2 livers compared with SD controls, restored by *in vivo* AT_1R blockade or antioxidant treatment.

Our findings also suggest that these deleterious effects of ANG II on hepatic mitochondria are mediated by increased ROS generation. Our results indicate that both increased activity of NADPH oxidase[18] and decreased activity of cytosolic Cu-ZnSOD (Figure 1E) contribute to mitochondrial oxidative stress in the Ren2 livers. Excessive ROS formation causes lipid peroxidation and release of reactive aldehydes such as 4-HNE. Lipid peroxidation has been shown to increase mitochondrial permeability, cause mtDNA depletion, and reduce gene transcription and peptide synthesis.[32–34] There is also evidence that 4-HNE inactivates mitochondrial respiratory chain and

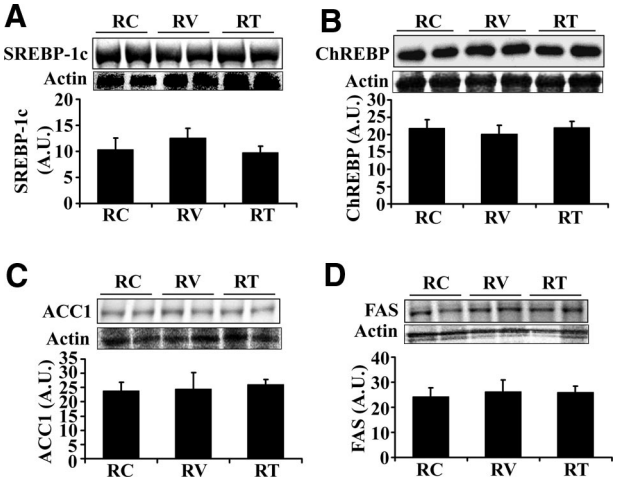

Figure 6. Effects of valsartan and tempol on hepatic lipogenic enzymes and transcription factors. Representative Western blot (**top**) and bar graphs (**bottom**) showed protein expression of active SREBP-1c (**A**), ChREBP (**B**), ACC1 (**C**), and FAS (**D**). The results are mean ± SEM for five rats for each group. There were no significant differences between groups ($P > 0.05$).

hampers electron flow of mitochondrial respiratory chain.[32–36] Inhibition/damage of mitochondrial respiratory chain complexes in turn further increases mitochondrial ROS production and accelerates mitochondrial oxidative stress.[37–39] The mechanisms for inactivation of mitochondrial respiratory chain complexes are possibly via tyrosine nitration.[40] In this regard, 4-HNE levels from Ren2 hepatic mitochondria were dramatically increased compared with SD livers (Figure 1D), and were substantially attenuated after valsartan or tempol treatment (Figure 4A).

Increased *de novo* fatty acid synthesis can also lead to hepatic steatosis. ACC1 and FAS are the key enzymes for *de novo* fatty acid syntheses and are mainly regulated by the transcription factors SREBP-1c and ChREBP.[41,42] Mice overexpressing SREBP-1c in the liver exhibit increased expression of FAS and develop fatty liver disease.[32] Liver-specific inhibition of ChREBP markedly decreases expression of ACC and FAS and attenuates hepatic steatosis in ob/ob mice.[31] SREBP-1c and ChREBP are inactive in the cytosol. When SREBP-1c (125 kDa) is cleaved by SREBP cleavage-activating protein (SCAP) via proteolytic processing, an active fragment (68 kDa) is generated. Regulation for ChREBP activation remains unclear, possibly through a mechanism of phosphorylation/dephosphorylation. Activated SREBP-1c and ChREBP translocate into the nucleus and regulate the expression of FAS and ACC1. Interestingly, there were no differences in the protein levels of active SREBP-1c and ChREBP between SD controls, untreated Ren2, and valsartan- or tempol-treated Ren2 rats (Figure 3, A and C, and Figure 6, A and B). Immunostaining revealed that SREBP-1c and ChREBP were predominately located in the cytoplasm with a similar staining pattern among SD controls, untreated Ren2, and treated Ren2 rats. ACC and FAS are the major enzymes that directly promote fatty acid synthesis. ACC1 catalyzes the carboxylation of acetyl-CoA to malonyl-CoA, which is converted into palmitate by FAS. There were no differences in the protein expression levels of ACC and FAS between SD controls, untreated Ren2, and valsartan- or tempol-treated Ren2 rats (Figure 3, E and F, and Figure 6, C and D). These results suggest that lipogenic pathway is not a contributor to ANG II-induced NAFLD in the Ren2 rat model.

In summary, we report here, for the first time, that elevated endogenous ANG II causes hepatic mitochondrial oxidative damage and impairs mitochondrial fatty acid β-oxidation contributing to the development of hepatic steatosis.

Acknowledgment

We thank Novartis Pharmaceutical Co. for providing valsartan.

References

1. Angulo P: Nonalcoholic fatty liver disease. N Engl J Med 2002, 346:1221–1231
2. Clark JM, Brancati FL, Diehl AM: Nonalcoholic fatty liver disease. Gastroenterology 2002, 122:1649–1657
3. Rector RS, Thyfault JP, Wei Y, Ibdah JA: Non-alcoholic fatty liver disease and the metabolic syndrome: an update. World J Gastroenterol 2008, 14:185–192
4. Wei Y, Rector RS, Thyfault JP, Ibdah JA: Nonalcoholic fatty liver disease and mitochondrial dysfunction. World J Gastroenterol 2008, 14:193–199
5. Monto A: Hepatitis C and steatosis. Semin Gastrointest Dis 2002, 13:40–46
6. Shimada M, Hashimoto E, Taniai M, Hasegawa K, Okuda H, Hayashi N, Takasaki K, Ludwig J: Hepatocellular carcinoma in patients with non-alcoholic steatohepatitis. J Hepatol 2002, 37:154–160
7. Neuschwander-Tetri BA, Brunt EM, Wehmeier KR, Oliver D, Bacon BR: Improved nonalcoholic steatohepatitis after 48 weeks of treatment with the PPAR-gamma ligand rosiglitazone. Hepatology 2003, 38:1008–1017
8. Sowers JR: Hypertension, angiotensin II, and oxidative stress. N Engl J Med 2002, 346:1999–2001
9. Bataller R, Sancho-Bru P, Gines P, Lora JM, Al-Garawi A, Sole M, Colmenero J, Nicolas JM, Jimenez W, Weich N, Gutierrez-Ramos JC, Arroyo V, Rodes J: Activated human hepatic stellate cells express the renin-angiotensin system and synthesize angiotensin II. Gastroenterology 2003, 125:117–125
10. Bataller R, Gabele E, Schoonhoven R, Morris T, Lehnert M, Yang L, Brenner DA, Rippe RA: Prolonged infusion of angiotensin II into normal rats induces stellate cell activation and proinflammatory events in liver. Am J Physiol 2003, 285:G642–G651
11. Helmy A, Jalan R, Newby DE, Hayes PC, Webb DJ: Role of angiotensin II in regulation of basal and sympathetically stimulated vascular tone in early and advanced cirrhosis. Gastroenterology 2000, 118:565–572
12. Kurita S, Takamura T, Ota T, Matsuzawa-Nagata N, Kita Y, Uno M, Nabemoto S, Ishikura K, Misu H, Ando H, Zen Y, Nakanuma Y, Kaneko S: Olmesartan ameliorates a dietary rat model of non-alcoholic steatohepatitis through its pleiotropic effects. Eur J Pharmacol 2008, 588:316–324
13. Muñoz MC, Argentino DP, Dominici FP, Turyn D, Toblli JE: Irbesartan restores the in-vivo insulin signaling pathway leading to Akt activation in obese Zucker rats. J Hypertens 2006, 24:1607–1617
14. Powell EE, Edwards-Smith CJ, Hay JL, Clouston AD, Crawford DH, Shorthouse C, Purdie DM, Jonsson JR: Host genetic factors influence disease progression in chronic hepatitis C. Hepatology 2000, 31:828–833
15. Ran J, Hirano T, Adachi M: Angiotensin II type 1 receptor blocker ameliorates overproduction and accumulation of triglyceride in the liver of Zucker fatty rats. Am J Physiol 2004, 287:E227–E232
16. Ran J, Hirano T, Adachi M: Chronic ANG II infusion increases plasma triglyceride level by stimulating hepatic triglyceride production in rats. Am J Physiol 2004, 287:E955–E961
17. Toblli JE, Munoz MC, Cao G, Mella J, Pereyra L, Mastai R: ACE inhibition and AT1 receptor blockade prevent fatty liver and fibrosis in obese Zucker rats. Obesity (Silver Spring) 2008, 16:770–776
18. Wei Y, Clark SE, Morris EM, Thyfault JP, Uptergrove GM, Whaley-Connell AT, Ferrario CM, Sowers JR, Ibdah JA: Angiotensin II-induced non-alcoholic fatty liver disease is mediated by oxidative stress in transgenic TG(mRen2)27(Ren2) rats. J Hepatol 2008, 49:417–428
19. de Cavanagh EM, Inserra F, Ferder M, Ferder L: From mitochondria to disease: role of the renin-angiotensin system. Am J Nephrol 2007, 27:545–553
20. Rector RS, Thyfault JP, Morris RT, Laye MJ, Borengasser SJ, Booth FW, Ibdah JA: Daily exercise increases hepatic fatty acid oxidation and prevents steatosis in Otsuka Long-Evans Tokushima fatty rats. Am J Physiol 2008, 294:G619–G626
21. Diehl AM: Fatty liver, hypertension, and the metabolic syndrome. Gut 2004, 53:923–924
22. Brookes MJ, Cooper BT: Hypertension and fatty liver: guilty by association? J Hum Hypertens 2007, 21:264–270
23. Donati G, Stagni B, Piscaglia F, Venturoli N, Morselli-Labate AM, Rasciti L, Bolondi L: Increased prevalence of fatty liver in arterial hypertensive patients with normal liver enzymes: role of insulin resistance. Gut 2004, 53:1020–1023
24. Jayasooriya AP, Mathai ML, Walker LL, Begg DP, Denton DA, Cameron-

Smith D, Egan GF, McKinley MJ, Rodger PD, Sinclair AJ, Wark JD, Weisinger HS, Jois M, Weisinger RS: Mice lacking angiotensin-converting enzyme have increased energy expenditure, with reduced fat mass and improved glucose clearance. Proc Natl Acad Sci USA 2008, 105:6531–6536
25. Diep QN, Benkirane K, Amiri F, Cohn JS, Endemann D, Schiffrin EL: PPAR alpha activator fenofibrate inhibits myocardial inflammation and fibrosis in angiotensin II-infused rats. J Mol Cell Cardiol 2004, 36:295–304
26. Ogihara T, Asano T, Ando K, Chiba Y, Sakoda H, Anai M, Shojima N, Ono H, Onishi Y, Fujishiro M, Katagiri H, Fukushima Y, Kikuchi M, Noguchi N, Aburatani H, Komuro I, Fujita T: Angiotensin II-induced insulin resistance is associated with enhanced insulin signaling. Hypertension 2002, 40:872–879
27. Caldwell SH, Swerdlow RH, Khan EM, Iezzoni JC, Hespenheide EE, Parks JK, Parker Jr WD: Mitochondrial abnormalities in non-alcoholic steatohepatitis. J Hepatol 1999, 31:430–434
28. Reddy JK, Rao MS: Lipid metabolism and liver inflammation. II. Fatty liver disease and fatty acid oxidation. Am J Physiol 2006, 290: G852–G858
29. Sanyal AJ, Campbell-Sargent C, Mirshahi F, Rizzo WB, Contos MJ, Sterling RK, Luketic VA, Shiffman ML, Clore JN: Nonalcoholic steatohepatitis: association of insulin resistance and mitochondrial abnormalities. Gastroenterology 2001, 120:1183–1192
30. Ibdah JA, Perlegas P, Zhao Y, Angdisen J, Borgerink H, Shadoan MK, Wagner JD, Matern D, Rinaldo P, Cline JM: Mice heterozygous for a defect in mitochondrial trifunctional protein develop hepatic steatosis and insulin resistance. Gastroenterology 2005, 128:1381–1390
31. Li H, Wang J, Wilhelmsson H, Hansson A, Thoren P, Duffy J, Rustin P, Larsson NG: Genetic modification of survival in tissue-specific knockout mice with mitochondrial cardiomyopathy. Proc Natl Acad Sci USA 2000, 97:3467–3472
32. Croteau DL, Stierum RH, Bohr VA: Mitochondrial DNA repair pathways. Mutat Res 1999, 434:137–148
33. Demeilliers C, Maisonneuve C, Grodet A, Mansouri A, Nguyen R, Tinel M, Letteron P, Degott C, Feldmann G, Pessayre D, Fromenty B: Impaired adaptive resynthesis and prolonged depletion of hepatic mitochondrial DNA after repeated alcohol binges in mice. Gastroenterology 2002, 123:1278–1290
34. Paradies G, Petrosillo G, Pistolese M, Ruggiero FM: The effect of reactive oxygen species generated from the mitochondrial electron transport chain on the cytochrome c oxidase activity and on the cardiolipin content in bovine heart submitochondrial particles. FEBS Lett 2000, 466:323–326
35. Chen J, Schenker S, Frosto TA, Henderson GI: Inhibition of cytochrome c oxidase activity by 4-hydroxynonenal (HNE). Role of HNE adduct formation with the enzyme subunits. Biochim Biophys Acta 1998, 1380:336–344
36. Chen J, Petersen DR, Schenker S, Henderson GI: Formation of malondialdehyde adducts in livers of rats exposed to ethanol: role in ethanol-mediated inhibition of cytochrome c oxidase. Alcohol Clin Exp Res 2000, 24:544–552
37. Doughan AK, Harrison DG, Dikalov SI: Molecular mechanisms of angiotensin II-mediated mitochondrial dysfunction: linking mitochondrial oxidative damage and vascular endothelial dysfunction. Circ Res 2008, 102:488–496
38. Muller FL, Liu Y, Van RH: Complex III releases superoxide to both sides of the inner mitochondrial membrane. J Biol Chem 2004, 279:49064–49073
39. Panov A, Dikalov S, Shalbuyeva N, Taylor G, Sherer T, Greenamyre JT: Rotenone model of Parkinson disease: multiple brain mitochondria dysfunctions after short term systemic rotenone intoxication. J Biol Chem 2005, 280:42026–42035
40. Han Z, Chen YR, Jones III CI, Meenakshisundaram G, Zweier JL, Alevriadou BR: Shear-induced reactive nitrogen species inhibit mitochondrial respiratory complex activities in cultured vascular endothelial cells. Am J Physiol 2007, 292:C1103–C1112
41. Dentin R, Benhamed F, Hainault I, Fauveau V, Foufelle F, Dyck JR, Girard J, Postic C: Liver-specific inhibition of ChREBP improves hepatic steatosis and insulin resistance in ob/ob mice. Diabetes 2006, 55:2159–2170
42. Horton JD, Goldstein JL, Brown MS: SREBPs: activators of the complete program of cholesterol and fatty acid synthesis in the liver. J Clin Invest 2002, 109:1125–1131